The electron - positron momentum density and Fermi surface in $\beta' - AgZn$

1996 J. Phys.: Condens. Matter 8 2413

(http://iopscience.iop.org/0953-8984/8/14/015)

J. Phys.: Condens. Matter **8** (1996) 2413–2423. Printed in the UK

The electron–positron momentum density and Fermi surface in β'-AgZn

A Waseda†, S Tanigawa†, H Nakashima†, X H Li†, K Oshima‡ and Y Matsuo§

† Institute of Materials Science, University of Tsukuba, Tsukuba, Ibaraki 305, Japan
‡ Institute of Applied Physics, University of Tsukuba, Tsukuba, Ibaraki 305, Japan
§ Department of Physics, Nara Women's University, Nara, Nara 630, Japan

Received 22 August 1995, in final form 2 January 1996

Abstract. We have determined the three-dimensional electron–positron momentum density for the ordered binary alloy β'-AgZn using two-dimensional angular correlation of positron annihilation radiation (2D-ACAR). The Fermi surface obtained from the momentum density is compared with the results from de Haas–van Alphen measurements and theoretical calculations. We have also observed the high-momentum components, and the enhancement effect on the momentum density.

1. Introduction

Intermetallic binary compounds such as β'-CuZn and β'-AgZn are of great interest since these compounds have the simplest type of ordering. These materials undergo a phase transition from a high-temperature random substitutional bcc (or A2) structure to a low-temperature ordered CsCl (or B2) structure. The silver–zinc binary alloy undergoes a second-order A2–B2 transition at 600 K. The ordered alloy β'-AgZn is known to be a Hume-Rothery compound. The valence electron concentration e/a is 1.5 and the first Brillouin zone is simple cubic. The B2 phase is stable at temperatures higher than 530 K and transforms into the ζ-phase of a partially ordered structure with trigonal symmetry. However, when the β-phase alloy is quenched into iced water, the transition into the ζ-phase is suppressed and a metastable β'-phase having the B2-type ordered structure is obtained. Unlike other Hume-Rothery phases, β'-AgZn does not undergo a martensitic transformation even if cooled down to liquid-helium temperature.

Electronic properties as well as structural properties of ordered and disordered phases have been studied by a number of authors. A theoretical calculation of the Fermi surface for ordered β'-CuZn alloy was performed by Arlinghauss [1]. Skriver has calculated the energy bands and the Fermi surface of β'-AgZn by the augmented-plane-wave (APW) method [2] and the results showed that β'-CuZn and β'-AgZn have similar Fermi surfaces and energy bands. Dunsworth and Jan obtained the shape of the first-zone hole surface via de Haas–van Alphen (dHvA) measurements [3], and the result showed an excellent agreement with Skriver's APW calculation.

In the present paper we have investigated the electronic structure of ordered β'-AgZn alloy in detail via two-dimensional angular correlation of positron annihilation radiation (2D-ACAR) measurements. From the measured electron momentum density, we determine

0953-8984/96/142413+11$19.50

the Fermi surface of β'-AgZn and compare the results with the theoretical calculation and the dHvA measurements. In addition, we discuss contributions from the reciprocal-lattice points, and the electron–positron many-body effect (enhancement effect) on the measured momentum density.

2. Experiments

The 2D-ACAR apparatus which was used in the present experiment consists of a pair of 128 $Bi_4Ge_3O_{12}$ (BGO) detectors. The angular resolution of the detector, D_D, is 0.75 mrad $\times$ 0.75 mrad. The distance between the sample and one of the detectors is 8 m. A radioactive isotope, ^{22}Na, with an activity of about 3×10^9 Bq was used as a positron source. The (001) plane of the single crystal of β'-AgZn was directed to the positron source in a vacuum. A magnetic field of 1.2 T, which was applied along the [001] direction, focused the positron beam from the positron source onto the specimen. The 2D-ACAR spectrum was measured on a 0.2 mrad $\times$ 0.2 mrad mesh in the momentum range of $\pm$22 mrad in two directions, one of which is the [001] direction, while the other is perpendicular to [001]. All of the measurements were performed at 32 K for the purpose of reducing the effect of residual momenta of thermalized positrons. The smearing of the angular resolution due to the momenta of positrons, D_T, is estimated to be 0.24 mrad in FWHM, assuming the effective mass of a positron to be twice the mass of a free electron. The smearing of the angular resolution due to the limited size of both the positron beam and the sample, D_S, is estimated to be 0.70 mrad. In the present experiment, D_S was determined by the size of the focused positron beam. The total resultant resolution in the direction parallel to the [001] axis is $(D_D^2+D_T^2)^{1/2} = 0.79$ mrad and that in the direction perpendicular to the [001] axis is $(D_D^2+D_T^2+D_S^2)^{1/2} = 1.05$ mrad. The 2D-ACAR spectra were measured for ten projections between [010] and [110] by rotating the sample around the [001] axis in 5° steps. The total accumulated coincidence counts was for each projection about 8×10^6 counts.

3. Data analysis

The 2D-ACAR spectrum

$$N(p_y, p_z) = \int \rho(\boldsymbol{p})\ \mathrm{d}p_x \tag{1}$$

is the projection of the electron–positron momentum density $\rho(\boldsymbol{p})$ onto the p_y–p_z plane, where $\boldsymbol{p}$ is the annihilating electron–positron pair momentum and p_x is the momentum component of the positrons parallel to the emitted γ-rays. From 2D-ACAR spectra for several different projections, we can reconstruct the full three-dimensional electron–positron momentum density by using the direct Fourier reconstruction technique [4, 5]. This technique is based on the following Fourier projection theorem:

$$\mathrm{FT}_2[N(p_x, p_y)] = \text{constant} \times B(\boldsymbol{r})|_{x=0} = (2\pi)^{-3/2} \iiint \rho(\boldsymbol{p})\mathrm{e}^{-\mathrm{i}\boldsymbol{p}\cdot\boldsymbol{r}}\ \mathrm{d}\boldsymbol{p}|_{x=0} \tag{2}$$

where $B(\boldsymbol{r})$ is the 3D Fourier transform of $\rho(\boldsymbol{p})$. The 2D-ACAR data which are measured for various directions are Fourier transformed into $B(\boldsymbol{r})$ by the fast Fourier transform, and then the interpolation of $B(\boldsymbol{r})$ onto a cubic grid is carried out. Finally, the 3D inverse Fourier transform of $B(\boldsymbol{r})$ yields the full 3D momentum density $\rho(\boldsymbol{p})$.

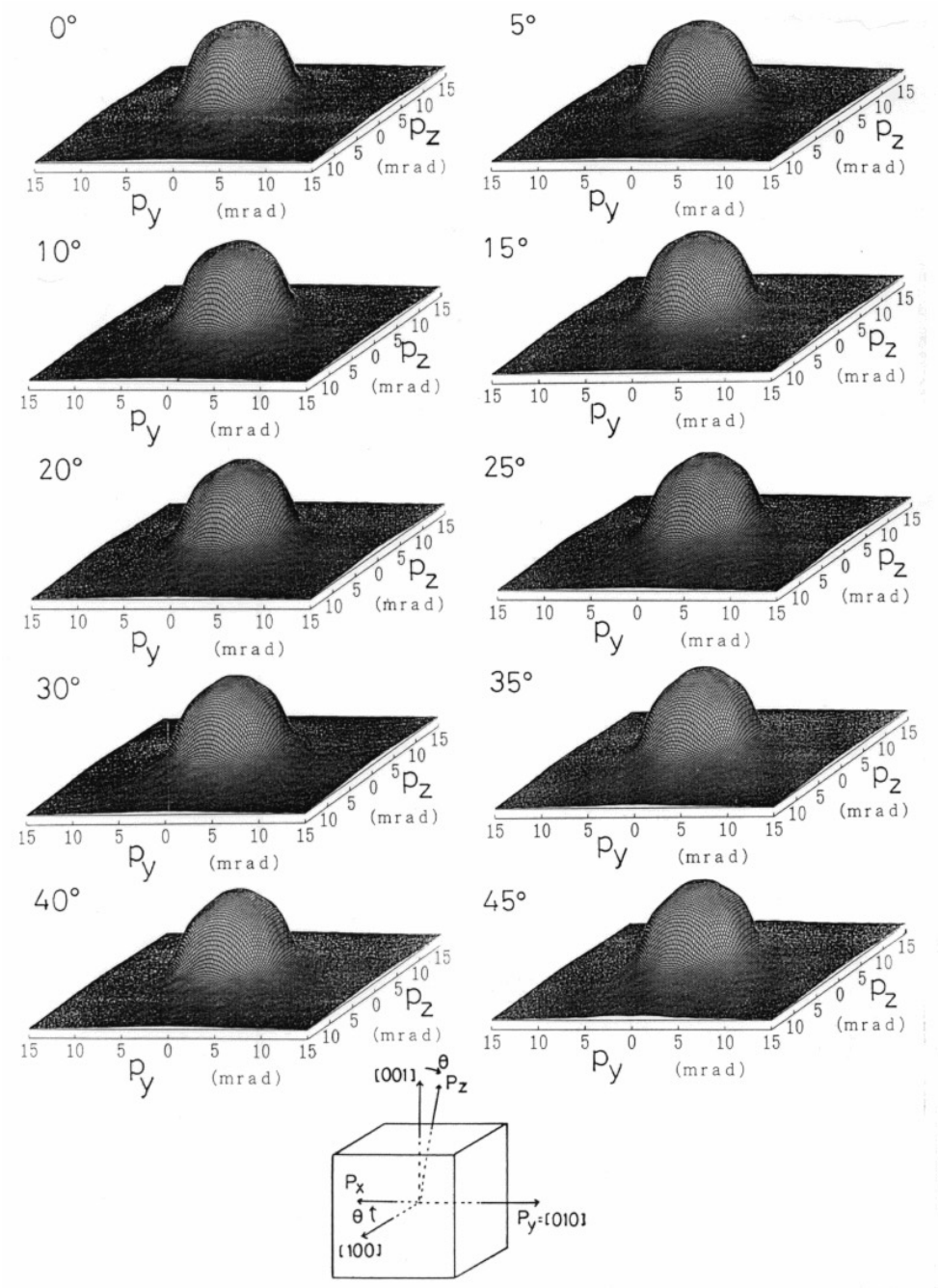

Figure 1. 2D-ACAR spectra for β'-AgZn. The angle denotes the deviation of the projection direction from [010].

In the independent-particle model, the electron–positron momentum density $\rho(\boldsymbol{p})$ can be expressed as

$$\rho(\boldsymbol{p}) = \text{constant} \times \sum_{n,\boldsymbol{k}}^{occ} \left| \int_V \mathrm{d}\boldsymbol{r}\ \psi_+(\boldsymbol{r})\psi_{n,\boldsymbol{k}}(\boldsymbol{r})\mathrm{e}^{-\mathrm{i}\boldsymbol{p}\cdot\boldsymbol{r}} \right|^2 \tag{3}$$

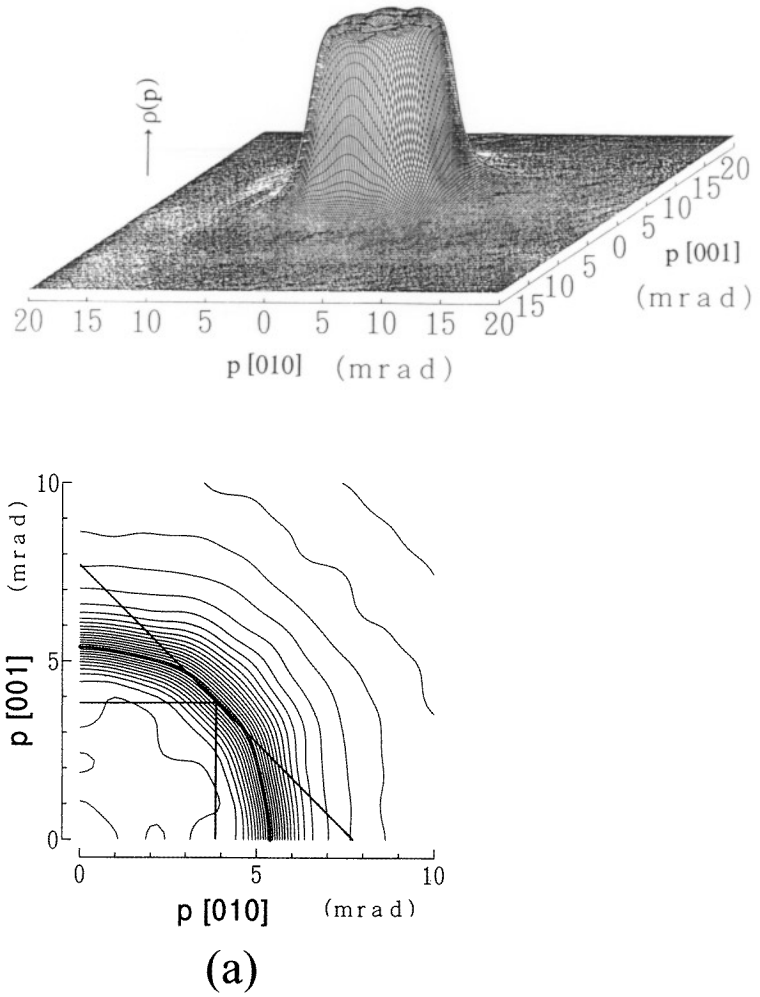

Figure 2. The electron–positron momentum density $\rho(\boldsymbol{p})$ for β'-AgZn on a central (100) plane (a) and a central (110) plane (b). The first and second Brillouin zone are also indicated.

where $\psi_{n,\boldsymbol{k}}(\boldsymbol{r})$ is the wavefunction of an electron, n is the band index, $\boldsymbol{k}$ is the wave vector, $\psi_{+}(\boldsymbol{r})$ is the wavefunction of a thermalized positron ($\boldsymbol{k} = 0$) and V is the crystal volume. The summation is taken over all occupied electron states.

The $\boldsymbol{p}$-space distribution $\rho(\boldsymbol{p})$ has extra contributions to the Fermi surface around the reciprocal-lattice points. In order to determine the precise Fermi surface, we folded back the $\boldsymbol{p}$-space distribution $\rho(\boldsymbol{p})$ into the $\boldsymbol{k}$-space using the Lock–Crisp–West (LCW) [6] folding procedure. This procedure is a periodical superposition of $\rho(\boldsymbol{p})$ on every reciprocal-lattice point as given by

$$n(\boldsymbol{k}) = \sum_{\boldsymbol{G}_j} \rho(\boldsymbol{p} + \boldsymbol{G}_j) \tag{4}$$

where $\boldsymbol{G}_j$ is the jth reciprocal-lattice vector and $\boldsymbol{k}$ is the wave vector defined within the first Brillouin zone. On the basis of the Bloch theorem, the $\boldsymbol{k}$-space distribution $n(\boldsymbol{k})$ can

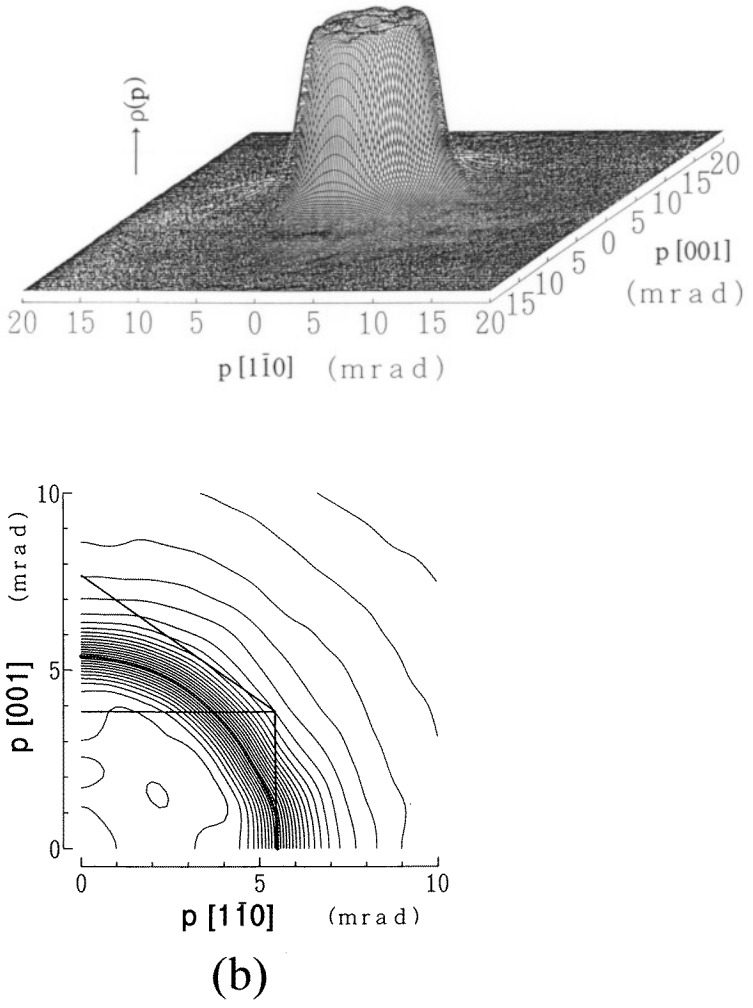

Figure 2. (Continued)

be described as

$$n(\boldsymbol{k}) = \text{constant} \times \sum_{n,\boldsymbol{k}} \theta(E_F - E_{n,\boldsymbol{k}}) \int_{cell} \mathrm{d}\boldsymbol{r}\ |\psi_+(\boldsymbol{r})|^2 |\psi_{n,\boldsymbol{k}}(\boldsymbol{r})|^2 \tag{5}$$

where E_F is the Fermi energy, $E_{n,\boldsymbol{k}}$ is the energy of the electron for the state $\psi_{n,\boldsymbol{k}}(\boldsymbol{r})$ and $\theta(E_F - E_{n,\boldsymbol{k}})$ is a step function defined as follows:

$$\theta(E_F - E_{n,\boldsymbol{k}}) = \begin{cases} 1 & E_F \geqslant E_{n,\boldsymbol{k}} \\ 0 & E_F < E_{n,\boldsymbol{k}}. \end{cases} \tag{6}$$

Therefore, $n(\boldsymbol{k})$ should have breaks corresponding to the Fermi surface edge. If the density of positrons can be assumed to be spatially uniform, the integral in equation (5) is equal to unity for occupied electron states. Even in the general case where the density of positrons is not uniform, the $\boldsymbol{k}$-dependence of the integral still seems to be not so large that the breaks in $n(\boldsymbol{k})$ can indicate the location of Fermi surface in $\boldsymbol{k}$-space.

4. Results and discussion

Figure 1 shows ten different 2D-ACAR spectra $N(p_y, p_z)$ for ordered β'-AgZn. All spectra with a hemispherical shape suggest that the distortion from a nearly-free-electron model is small. This experimental result is in good agreement with the theoretical result [2] that the Fermi surface can be understood in terms of a nearly-free-electron model.

We reconstructed the three-dimensional momentum density $\rho(\boldsymbol{p})$ from ten different 2D-ACAR spectra. The reconstruction was performed up to 20 mrad. Figure 2 shows $\rho(\boldsymbol{p})$ on central (100) and (110) planes. These distributions are almost isotropic, but have anisotropy at the M points (the distance ΓM is 5.46 mrad). It is considered that this anisotropy reflects the neck at the M point. By finding the momentum $\boldsymbol{p}_F$ satisfying the condition that $|\nabla\rho(\boldsymbol{p})|$ has a maximum along the radial direction, we determined the Fermi surface of β'-AgZn in the extended-zone scheme. The Fermi surface determined by this procedure in the extended zone is only an approximation because of the contribution of reciprocal-lattice points at large momentum.

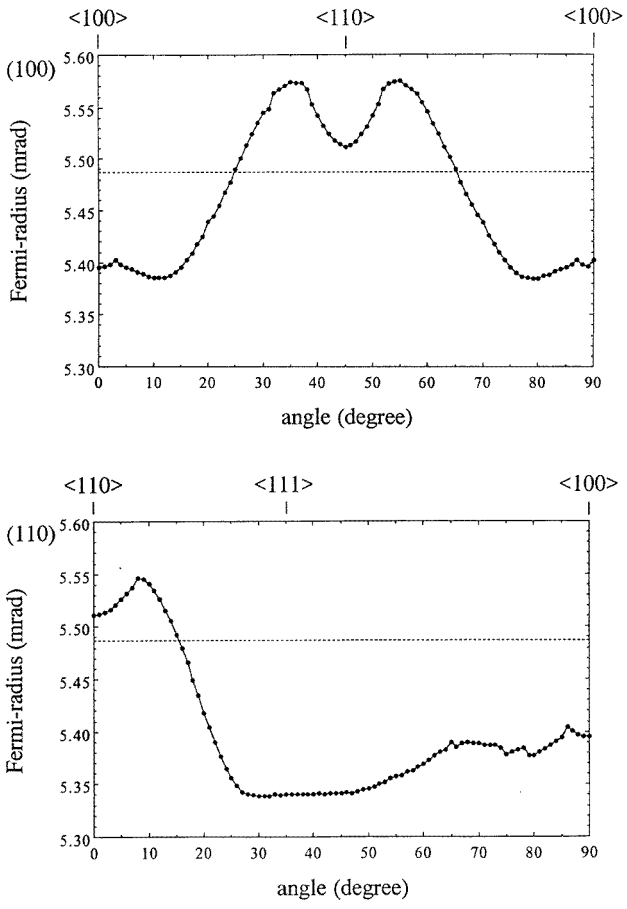

Figure 3. The Fermi momentum obtained from the electron–positron momentum density $\rho(\boldsymbol{r})$. The horizontal dotted line represents the free-electron Fermi radius. The experimental resolution of 1 mrad corresponds to the spread of about 11° in the angle at the free-electron Fermi radius.

Figure 3 shows the Fermi momentum of β'-AgZn in an extended zone on central (100) and (110) planes. The free-electron Fermi radius p_F for β'-AgZn is calculated to be 5.487 mrad, assuming that there are three conduction electrons per primitive cell. The deviation of the Fermi momentum from the free-electron Fermi radius is within the range -2.7% to $+1.5\%$.

In order to discuss the precise Fermi surface, we folded back the $\boldsymbol{p}$-space data $\rho(\boldsymbol{p})$ into the $\boldsymbol{k}$-space momentum density $n(\boldsymbol{k})$ using the LCW folding procedure. Figure 4 shows the normalized $n(\boldsymbol{k})$ along the principal symmetry lines normalized as follows:

$$n(\boldsymbol{k}) \Big/ \left(\int n(\boldsymbol{k})\ \mathrm{d}k \Big/ \int \mathrm{d}k \right) \times 100(\%)\ . \tag{7}$$

It is expected from the calculation that at X and M points there are electron surfaces and at R and Γ points there are hole surfaces.

Table 1. Extremal cross sectional areas (in units of $(2\pi/a)^2$).

	2D-ACAR	dHvA [3]	APW [2]	Free electron [7]
A_1^R	0.169	0.1783	0.184	0.203
A_2^R	—	—	0.222	0.203
A_2^Γ	0.354	—	—	0.417
B_1^R	0.138	0.1304	0.130	0.123
B_2^X	0.281	0.2600	0.260	0.292
B_2^M	0.212	0.1747	0.136	0.013

We shall discuss the Fermi surface topology for β'-AgZn in detail. Theoretical calculations and dHvA measurements show that in the first zone the Fermi surface has a hole sheet which has the shape of an octahedron centred at the R point, and that in the second zone it has the form of convex lenses perturbed by necks lying perpendicular to the ⟨110⟩ direction. We determined the Fermi surface of β'-AgZn in the reduced zone as the loci of the local maximum of $|\boldsymbol{\nabla}\rho(\boldsymbol{p})|$. Figure 5 shows the Fermi surface obtained by this experiment on the R-centred (110) plane (a), the R-centred (100) plane (b) and the Γ-centred (100) plane (c), respectively. The cross sectional areas of the Fermi surface of β'-AgZn obtained from this experiment, the dHvA experiment [3], the APW calculation [2] and the free-electron model [7] are also listed in table 1. The labels in the table correspond to those given by Jan *et al* [7], i.e., A and B stand for the normal directions ⟨100⟩ and ⟨110⟩, respectively, the subscript represents the band number, and the superscript represents the central point. First, we discuss the first-zone hole surface. There is a hole sheet centred at the R point, as shown in figure 5(a). The 2D-ACAR result for B_1^R is in good agreement with the results from the APW calculation and the dHvA experiment, and that for A_1^R agrees with the dHvA experimental result but does not agree with that obtained by the APW calculation. As for the second-zone Fermi surface, the extremal cross sectional area of B_2^X agrees with the result from the APW calculation and that from the dHvA experiment. On the other hand, the cross sectional areas of B_2^M from 2D-ACAR and dHvA experiments do not agree with that from the APW calculation. We could not determine the cross section of A_1^R, because at the R point the Fermi surface has both a first-zone hole A_1^R and a second-zone hole orbit A_2^R. The 2D-ACAR results are in good agreement with those from the dHvA experiment, but there is a small discrepancy between our results and those from the theoretical calculation.

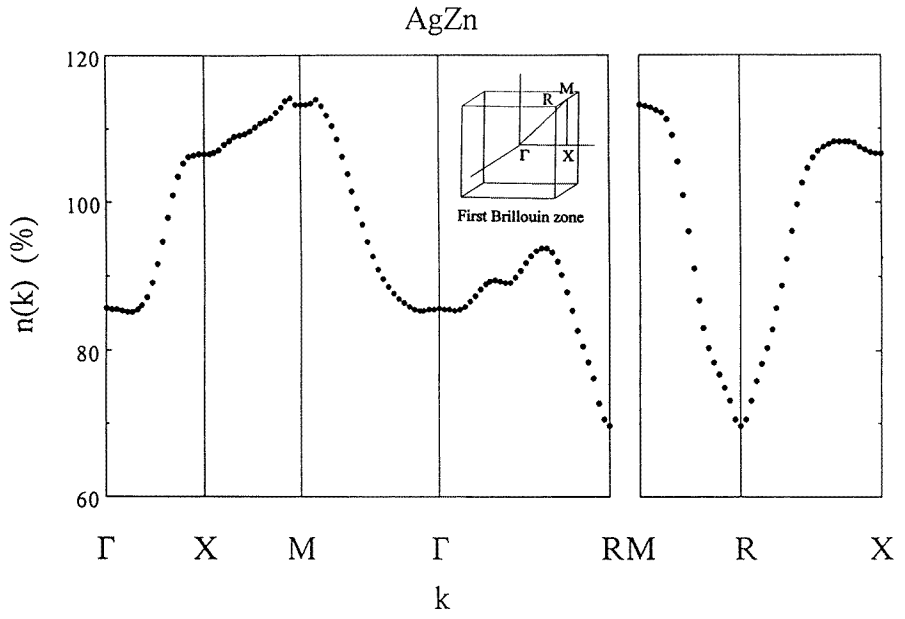

Figure 4. The reduced-zone electron–positron momentum density $n(\boldsymbol{k})$ for β'-AgZn for various symmetry points and symmetry axes. The average of $n(\boldsymbol{k})$ is 100%.

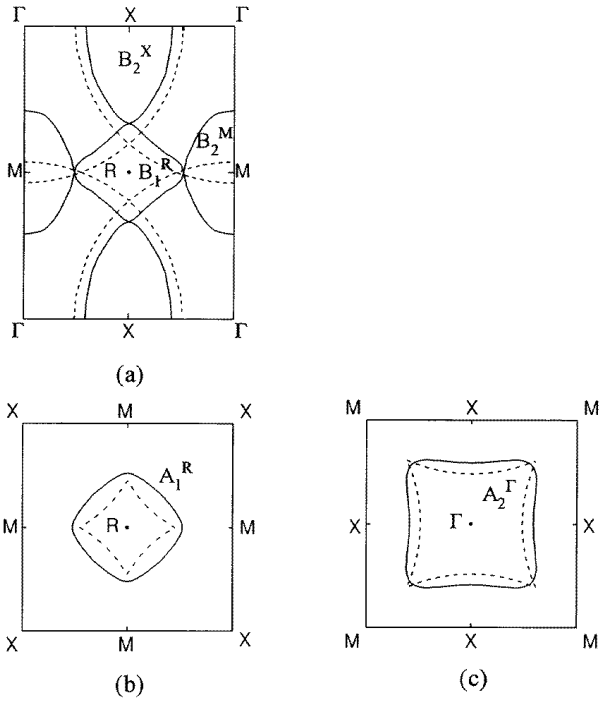

Figure 5. The Fermi surface in the reduced zone for β'-AgZn on (110) centred on R (a), on (100) centred on R (b) and on (100) centred on Γ (c). Solid line: 2D-ACAR experiment. Dotted line: free-electron model.

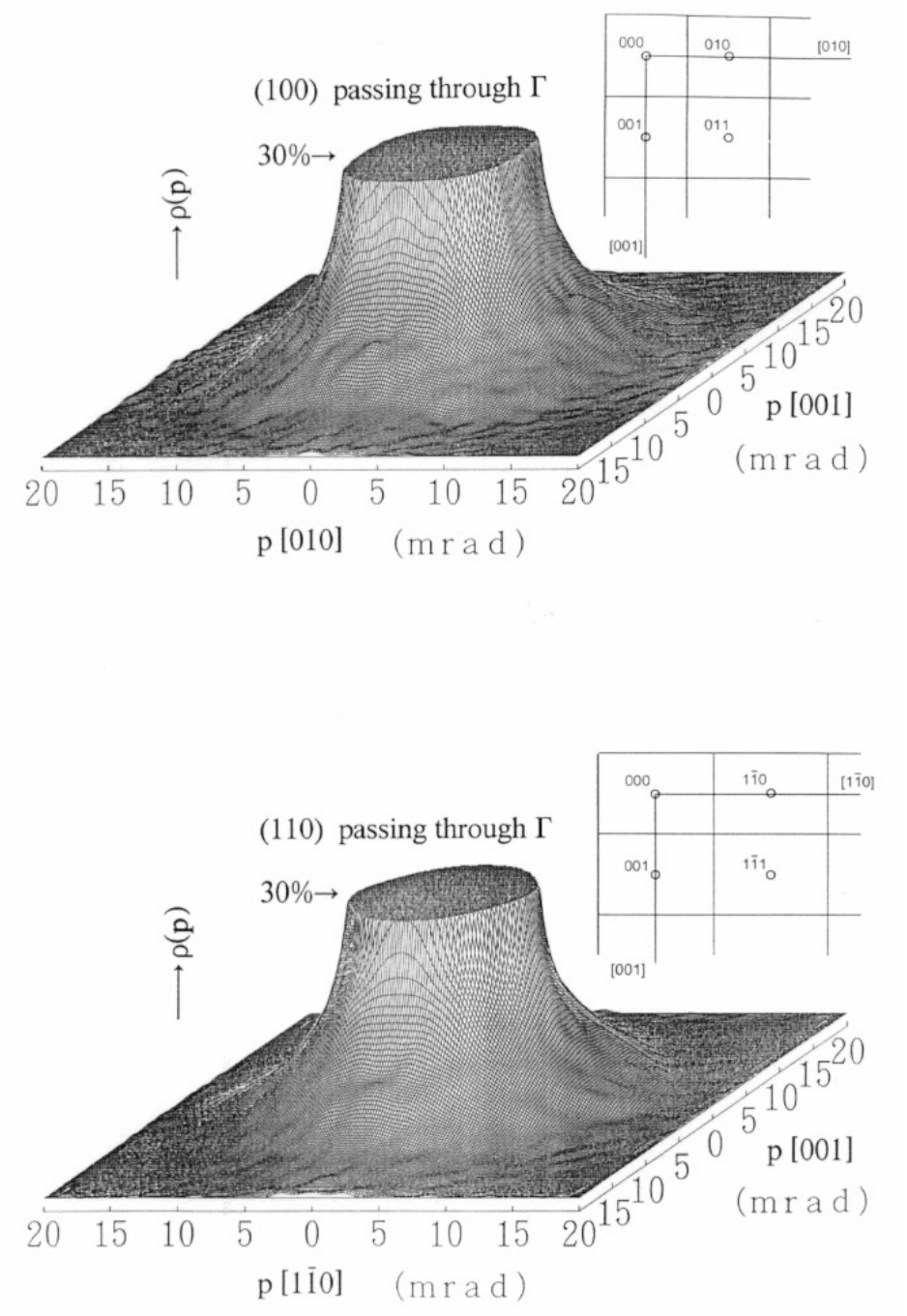

Figure 6. The lower part of the electron–positron momentum density $\rho(\boldsymbol{p})$ on the central (100) and (110) planes.

In the region of momentum higher than the Fermi momentum, the value of $\rho(\boldsymbol{p})$ is the sum of both core and the reciprocal-lattice contributions, which are called high-momentum

components (HMC). In order to observe $\rho(\boldsymbol{p})$ in the high-momentum region, we enlarged $\rho(\boldsymbol{p})$ on the (100) and (110) planes as shown in figure 6. It is noted that the contributions of $\boldsymbol{G}_{001} = (0, 0, 2\Gamma\mathrm{X})$ ($\Gamma\mathrm{X} = 3.86$ mrad) are clearly seen on the (110) plane.

Table 2. Enhancement parameters, b/a, c/a and $(b + c)/a$, determined from the electron–positron momentum density $\rho(\boldsymbol{p})$ along the [100], [110] and [111] directions, compared with the theoretical results of Kahana [8] and Arponen and Pajanne [9].

	b/a	c/a	$(b+c)/a$
[100]	0.24	0.14	0.38
[110]	0.24	0.20	0.44
[111]	0.25	0.15	0.40
Kahana	0.19	0.13	0.32
Arponen and Pajanne	0.12	0.11	0.23

The electron–positron momentum density $\rho(\boldsymbol{p})$ inside the Fermi surface is not constant but depends on $\boldsymbol{p}$. This momentum dependence is called the enhancement effect, and is represented by Kahana [8] for an interacting gas as

$$\varepsilon = \frac{\rho_V(\boldsymbol{p})}{\rho_{IPM}(\boldsymbol{p})} = a\left(1 + \frac{b}{a}\left(\frac{p}{p_F}\right)^2 + \frac{c}{a}\left(\frac{p}{p_F}\right)^4\right) \tag{8}$$

where $\rho_V(\boldsymbol{p})$ is the valence electron contribution, $\rho_{IPM}(\boldsymbol{p})$ is the momentum density in the IPM, and a, b and c are constants. In order to determine the enhancement parameters b/a and c/a, we must subtract the core-electron contribution from the experimental $\rho(\boldsymbol{p})$. We assumed the core-electron background to be a Gaussian for simplicity, and fitted the Gaussian function from the data above 10 mrad and subtracted the Gaussian part from the data, where the statistical error is about 2% at 10 mrad. Then we fitted the data to equation (8) with convolution of the angular resolution function. We used the free-electron value of 5.487 mrad as the Fermi momentum p_F and assumed $\rho_{IPM}(\boldsymbol{p})$ to be constant. The fitted parameters for along three directions are given in table 2 and compared with the Kahana, and Arponen and Pajanne [9] theoretical values which are interpolated for the electron density $r_s = 2.55$ au. It is found that all of the present experimental values are greater than the theoretical values, the values of b/a are the same for all directions, and the values of c/a for the $\langle 100\rangle$ direction are greater than those for $\langle 100\rangle$ and $\langle 110\rangle$ directions. It is considered that the anisotropy for the $\langle 110\rangle$ direction is related to the fact that the Fermi momentum for the $\langle 110\rangle$ direction is very close to the Brillouin zone boundary, and the electrons cannot be considered as free electrons. The Kahana-like theories describe the positron–electron many-body effects reasonably well except as regards the condition that the electron does not behave as a free electron.

5. Conclusions

In the present work, the three-dimensional electron–positron momentum density $\rho(\boldsymbol{p})$ of β'-AgZn was measured by means of 2D-ACAR. We reduced $\rho(\boldsymbol{p})$ to the reduced zone momentum density $n(\boldsymbol{k})$, and determined the Fermi surface of β'-AgZn. The agreement between the 2D-ACAR and dHvA results is excellent. However, a small discrepancy is seen between our results and the results from the theoretical calculations. The high-momentum components were observed in the measured $\rho(\boldsymbol{p})$. The enhancement parameters determined from the present experimental data are greater than the theoretical values and have anisotropy

for the ⟨110⟩ direction. The validity of 2D-ACAR technique as applied to ordered β'-AgZn was experimentally examined, and the shape and position of the Fermi surface obtained from the 2D-ACAR spectra agree in general with the results from dHvA experiments and theoretical calculations.

Acknowledgments

This work was supported in part by a Grant-in-Aid for Scientific Research from the Ministry of Education, Science and Culture and by a NEDO Grant for International Cooperative Research.

References

[1] Arlinghauss F J 1969 *Phys. Rev.* **186** 609
[2] Skriver H L 1973 *Phys. Status Solidi* b **58** 721
[3] Dunsworth A E and Jan J P 1973 *J. Low Temp. Phys.* **13** 53
[4] Suzuki R and Tanigawa S 1989 *Positron Annihilation* ed L Dorikens-Vanpraet, M Dorikens and D Segers (Singapore: World Scientific) p 626
[5] Suzuki R, Osawa M, Tanigawa S, Matsumoto M and Shiotani N 1989 *J. Phys. Soc. Japan* **58** 3251
[6] Lock D G, Crisp V H C and West R N 1973 *J. Phys. F: Met. Phys.* **3** 561
[7] Jan J P, Pearson W B and Saito Y 1967 *Proc. R. Soc.* A **297** 275
[8] Kahana S 1963 *Phys. Rev.* **129** 1622
[9] Arponen J and Pajanne E 1979 *J. Phys. F: Met. Phys.* **9** 2359